ANALYSIS OF PHASE DISTRIBUTION PHENOMENA IN MICROGRAVITY ENVIRONMENTS

Dr. R.T. Lahey, Jr.
Dr. F. Bonetto
Center for Multiphase Research
Rensselaer Polytechnic Institute
Troy, NY 12180-3590

CMR
CMR
CMR

INTRODUCTION

In the past one of NASA's primary emphasis has been on identifying single and multiphase flow experiments which can produce new discoveries that are not possible except in a microgravity environment. While such experiments are obviously of great scientific interest, they do not necessarily provide NASA with the ability to use multiphase processes for power production and/or utilization in space.

The purpose of the research presented in this paper is to demonstrate the ability of multidimensional two-fluid models for bubbly two-phase flow to accurately predict lateral phase distribution phenomena in microgravity environments. If successful, this research should provide NASA with mechanistically-based analytical methods which can be used for multiphase space system design and evaluation, and should be the basis for future shuttle experiments for model verification.

DISCUSSION

During the last decade mechanistically-based multidimensional two-fluid models have been developed and successfully applied to the prediction of bubbly two-phase flows. It appears that these models should also work in microgravity environments, however this still needs to be verified.

To this end experiments are being conducted within Rensselaer's Center for Multiphase Research (CMR). In particular, microgravity conditions have been simulated using neutral buoyant polystyrene spheres, and future experiments will be performed in which neutral buoyant oil droplets are immersed in flowing water.

The purpose of this paper is to present the progress to date in the analytical modeling of dispersed flows and to present the solid/fluid data which has been taken to support these modeling efforts.

We will begin by summarizing the multidimensional two-fluid model and then will present the solid/fluid data which has been acquired in this program.

ANALYSIS

The analysis of multidimensional two-phase flow can be done using two-fluid models and associated computational fluid dynamic (CFD) numerical evaluation algorithms (eg, PHOENICS or FLOW3D). For example, the evaluation of adiabatic bubbly two-phase flows are governed by the two-fluid conservation equations for mass and momentum. These balance equations can be derived using ensemble averaging techniques [Lahey & Drew, 1992].

TWO-PHASE FLOW BALANCE EQUATIONS

The three dimensional balance equations for adiabatic two-phase flow are:

Mass Conservation

$$\frac{\partial[\alpha_k \rho_k]}{\partial t} + \nabla \bullet [\alpha_k \rho_k \underline{v}_k] = 0 \qquad (1)$$

where α_k is the volume fraction, ρ_k is the density, and $\underline{v}_k$ is the average velocity of phase-k, respectively.

Momentum Conservation

$$\frac{\partial[\alpha_k \rho_k \underline{v}_k]}{\partial t} + \nabla\bullet[\alpha_k \rho_k \underline{v}_k \underline{v}_k] = -\nabla[\alpha_k p_k] + \nabla\bullet\left[\alpha_k \left(\underline{\underline{\tau}}_k + \underline{\underline{\tau}}_k^{Re}\right)\right] + \alpha_k \rho_k \underline{g} + \underline{M}_k \qquad (2)$$

where $\underline{M}_k$ is the interfacial force density, p_k is the static pressure, $\underline{\underline{\tau}}_k$ is the viscous stress tensor, and $\underline{\underline{\tau}}_k^{Re}$ is the Reynolds stress on phase-k, respectively.

The interfacial jump condition for momentum is:

$$\underline{M}_v + \underline{M}_\ell = \underline{m}_i^\sigma \qquad (3)$$

where, m_i^σ is the interfacial momentum source density due to surface tension effects (eg, Marangoni forces).

CLOSURE

For dispersed spherical particles (eg, bubbles), we may use the interfacial transfers developed by Park [1992]. It is conventional to partition the interfacial force density ($\underline{M}_k$) into drag (d) and nondrag (nd) components:

$$\underline{M}_v = \underline{M}_v^{(d)} + \underline{M}_v^{(nd)}. \qquad (4)$$

We assume the following form of the interfacial drag law:

$$\underline{M}_\ell^{(d)} = -\underline{M}_v^{(d)} = \frac{1}{8}\rho_\ell C_D \, |\underline{v}_r| \underline{v}_r \, A_i''' \qquad (5)$$

where, $\underline{v}_r = \underline{v}_v - \underline{v}_\ell$, and for spherical monodispersed bubbles, $A_i''' = 6\alpha_v/\bar{D}_b$ is the interfacial area density of the interface between the continuous phase and the dispersed bubbles. Assuming the validity of inviscid flow theory for the continuous phase the non-drag interfacial force density for the continuous phase is, using cell-model averaging techniques [Park, 1992], [Lopez de Bertodano, 1992]:

$$\underline{M}_\ell^{(nd)} = -\underline{M}_v^{(nd)} = -p_{\ell_i}\nabla\alpha_v + \alpha_v\rho_\ell C_{vm}\underline{a}_{vm} + \alpha_v\rho_\ell C_1 \underline{v}_r\bullet\nabla\underline{v}_r$$

$$+ \alpha_v \rho_\ell C_2 \left[\underline{v}_r \bullet (\nabla \underline{v}_r^T) + (\nabla \bullet \underline{v}_r) \underline{v}_r \right] + b_s \rho_\ell \underline{v}_r \bullet \underline{v}_r \nabla \alpha_v$$

$$+ a_s \rho_\ell \underline{v}_r \bullet \nabla \alpha_v \underline{v}_r + \alpha_v \rho_\ell C_{rot} \underline{v}_r \times \nabla \times \underline{v}_v + \alpha_v \rho_\ell C_L \underline{v}_r \times \nabla \times \underline{v}_\ell \tag{6}$$

Also, for a spherical dispersed phase the interfacial force required to have the bubbles maintain a spherical shape is [Park, 1992]:

$$\underline{m}_i^s = \nabla \bullet [\alpha_v \underline{\underline{\sigma}}_s] = \nabla \bullet \left[\alpha_v \rho_\ell \left(\hat{a}_s \underline{v}_r \underline{v}_r + \hat{b}_s \underline{v}_r \bullet \underline{v}_r \underline{\underline{I}} \right) \right] \tag{7}$$

Also, for the interfacial averaged-pressure, we have [Park, 1992]:

$$p_{\ell_i} = p_\ell + C_p \rho_\ell |\underline{v}_r|^2 \tag{8}$$

For bubbly two-phase flows the total Reynolds stress tensor for the continuous liquid phase is given by superposition as,

$$\underline{\underline{\tau}}_\ell^{Re} = \underline{\underline{\tau}}_{\ell(BI)}^{Re} + \underline{\underline{\tau}}_{\ell(SI)}^{Re} \tag{9}$$

where, for bubbly two-phase flows the bubble-induced shear stress is given by cell-model averaging [Lopez de Bertodano, 1992] as:

$$\alpha_\ell \underline{\underline{\tau}}_{\ell(BI)}^{Re} = - \alpha_v \rho_\ell \left[a_\ell \underline{v}_r \underline{v}_r + b_\ell \underline{v}_r \bullet \underline{v}_r \underline{\underline{I}} \right] \tag{10}$$

We note that $\underline{\underline{\tau}}_{\ell(SI)}^{Re}$ is the shear-induced Reynolds stress which may come from a classical k-ε model and an algebraic stress law [Rodi, 1984].

For the inertial coupling of all dispersed/continuous phase interactions we have [Park, 1992]:

$$C_{vm} = C_L + C_{rot} = \frac{1}{2}, C_L = C_{rot} = \frac{1}{4}, C_1 = \frac{5}{4},$$
$$C_2 = -\frac{9}{20}, a_s = \hat{a}_s = -\frac{9}{20}, b_s = \hat{b}_s = \frac{3}{20}, C_p = \frac{1}{4}, a_\ell = -\frac{1}{20}, b_\ell = -\frac{3}{20}. \tag{11}$$

It is significant to note that there are no arbitrary constants in the two-fluid model, however data on the interfacial drag coefficient, C_D, and the lateral lift coefficient, C_L, indicate that they should be a function of Reynolds number.

MODEL ASSESSMENT

The two-fluid model given in Eqs. (1)-(11) has been assessed against a wide variety of terrestrial air/water bubbly flow data.

Figure-1 shows a comparison of the two-fluid model with the air/water bubbly upflow void fraction data of Serizawa [1974]. Good agreement can be seen. Figure-2 shows that the turbulence model being used does a good job of predicting the measured nonisotropic turbulent structure of Serizawa. Similarly, Figure-3 shows that the model predicts Serizawa's two-phase Reynolds stress data and that, unlike fully developed single-phase flow (ie, $j_v = 0$), the two-phase Reynolds stress distribution is not linear in the radial direction (since the radial void distribution is not linear).

Figure-4 is very exciting because it shows that the same multidimensional two-fluid model which was used to predict Serizawa's bubbly upflow data is able to predict the air/water bubbly downflow data of Wang et al [1987]. Notice the lateral phase distribution in Figure-4 is completely different from Figure-1. This is due to the fact that the lateral lift force changes sign for downflows since the effect of buoyancy causes the relative velocity to change sign.

Figures-5&6 are perhaps the most impressive comparisons of all, since they show that the same multidimensional two-fluid model is also able to predict the lateral phase and velocity distribution in complex geometry conduits (ie, vertical air/water bubbly upflows in an isosceles triangular test section).

These data comparisons clearly indicate that the multidimensional two-fluid model given in Eqs. (1)-(11) is able to predict a wide range of adiabatic bubbly flow

data taken on earth. Moreover, since this model is based on first principles it should also be able to predict lateral phase distribution for bubbly flows in microgravity experiments.

EXPERIMENTS

In order to simulate microgravity bubbly flow data, a experiment has been performed using approximately 2 mm diameter expanded polystyrene spheres immersed in water. The specific gravity of these spheres was 1.03, thus they were essentially neutral buoyant.

Figure-7 is a schematic of the test loop. Figure-8 shows a schematic of the novel ventri-type phase separation device which was developed and used to avoid damage to the dispersed particles. Figure-9 is a schematic of the horizontal test section and the DANTEC three-dimensional laser Doppler anemometer (LDA) system which was used. It can be noted that the fiber optic laser transmitter/receiver heads were submerged in water and the tubular test section was constructed of fluorinated ethylene propylene (FEP) which has about the same index of refraction as water, thus no corrections for laser beam refraction were necessary.

Figure-10 presents the measured particle volume fraction distribution. These data were corrected for beam interruptions, etc. using the method of Alajbegović, et al [1994]. It should be noted when these data were integrated across the cross-section they agreed to within ±1% with the corresponding global volume fraction data, which were taken using quick closing valves (Figure-11).

Figures-12 & 13 show the Reynolds stress data for the dispersed particles and the continuous liquid phase (water), respectively, and figures-14 & 15 show data for the axial velocity fluctuations of the particles and the water, respectively. It can be seen that both data sets yield similar results.

Figure-16 gives data on the mean axial velocity of the particles and the liquid phase, respectively. It can be seen that these data are symmetric (as they should be for neutral buoyant particles) and that the relative velocity is negligible, as would be expected for bubbly flow in a microgravity environment. Hence, except for interfacial boundary condition differences between a bubble and a solid sphere, these data comprise an excellent basis for the assessment of the two-fluid model for use in microgravity environments.

MODEL ASSESSMENT

Figures-17 show good agreement between the multidimensional two-fluid model presented in Eqs. (1)-(11) and the solid/fluid data discussed herein.

Interestingly, it appears that the two-fluid model predictions agree better with the uncorrected particle volume fraction data than the corrected data. It is not completely clear at this time why this occurs, however the data correction method which we used [Alajbegović et al, 1994] implicitly assumes that the dispersed particles are opaque, while the actual particles were translucent, thus it is likely that the data correction applied was inappropriate. This issue will require further study and the results of this study will be reported subsequently.

Nevertheless, it appears that the essential physics of lateral phase separation is captured by the two-fluid model, and thus it should be appropriate for microgravity environments.

Since solid particles satisfy the no slip condition at their surface while vapor bubbles and liquid droplets do not, a series of experiments using neutral buoyant oil droplets immersed in water will also be performed and the two-fluid model will also be assessed against these data. An oil/water loop, shown schematically in Figure-18, has been designed and built and system shakedown is under way.

SUMMARY & CONCLUSIONS

It has been shown that a mechanistically-based, multidimensional two-fluid model has been developed, and that it is capable of predicting a wide range of terrestrial bubbly flow data.

An experiment has been performed in which detailed multidimensional measurements have been made for turbulent solid/fluid flows which simulate bubbly flows in a microgravity environment (ie, the spherical particles used had essentially the same density as water and thus the buoyancy term was eliminated).

Initial comparisons between the solid/fluid data and the multidimensional two-fluid model showed good agreement and imply the validity of this model for microgravity environments.

REFERENCES

Alajbegović, A., Assad, A., Bonetto, F. and Lahey, R.T., Jr., "Phase Distribution and Turbulence Structure for Solid/Fluid Upflow in a Pipe," Approved for publication, *Int. J. Multiphase Flow*, 1994.

Lahey, R.T., Jr. and Drew, D.A., "On the Development of Multidimensional Two-Fluid Models for Vapor/Liquid Two-Phase Flows," *Chem. Eng. Comm.*, Vol-118, 1992.

Lopez de Bertodano, M., "Turbulent Bubbly Two-Phase Flow in a Triangular Duct," Ph.D. Thesis, Nuclear Engineering & Science, Rensselaer Polytechnic Institute, Troy, NY, 1992.

Park, J-W., "Void Wave Propagation in Two-Phase Flow," Ph.D. Thesis, Nuclear Engineering & Science, Rensselaer Polytechnic Institute, Troy, NY, 1992.

Serizawa, A., "Fluid-Dynamic Characteristics of Two-Phase Flow," Ph.D. Thesis, University of Kyoto, Japan, 1974.

Wang, S.K., Lee, S.J., Lahey, R.T., Jr. and Jones, O.C., Jr., "3-D Turbulence Structure and Phase Distribution Measurements in Bubbly Two-Phase Flows," *Int. J. Multiphase Flow*, Vol-13, No. 3, 1987.

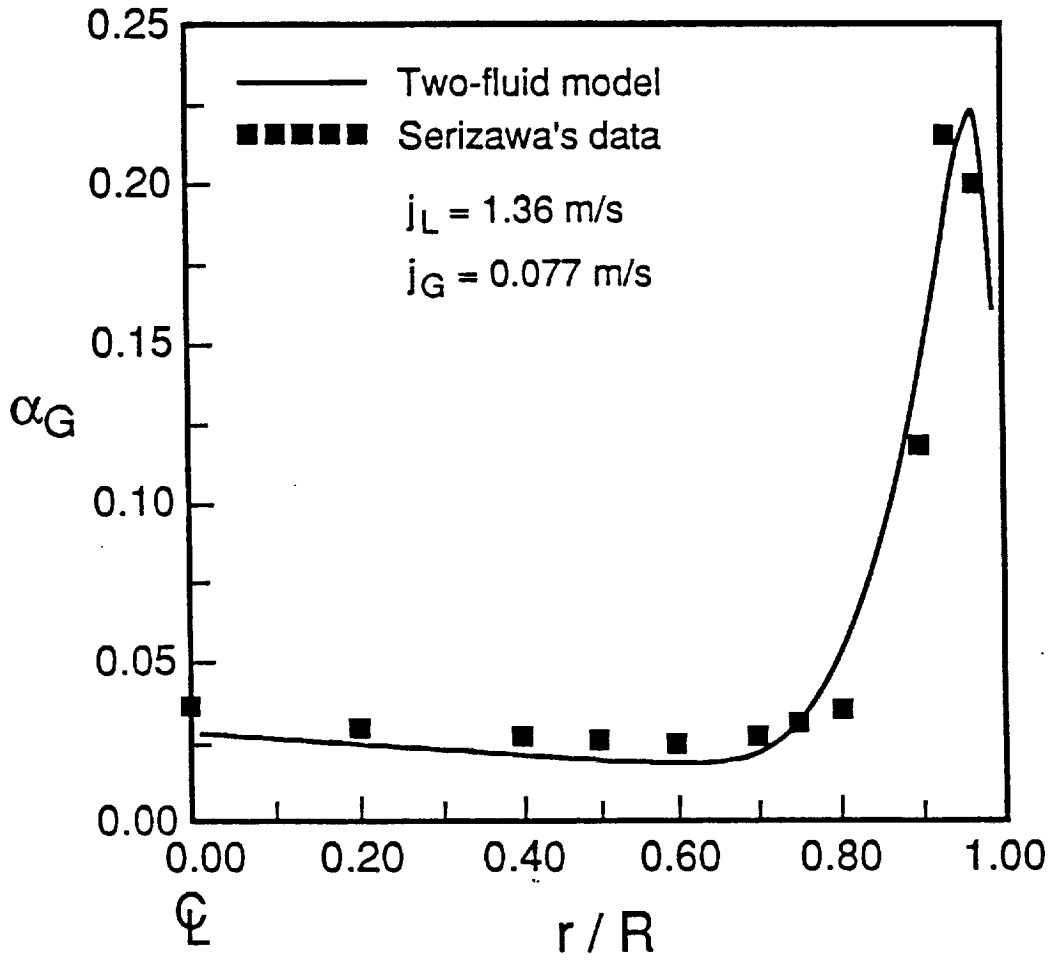

Comparison with Serizawa's data [1986]: void fraction distribution (C_L = 0.1)

Figure-1

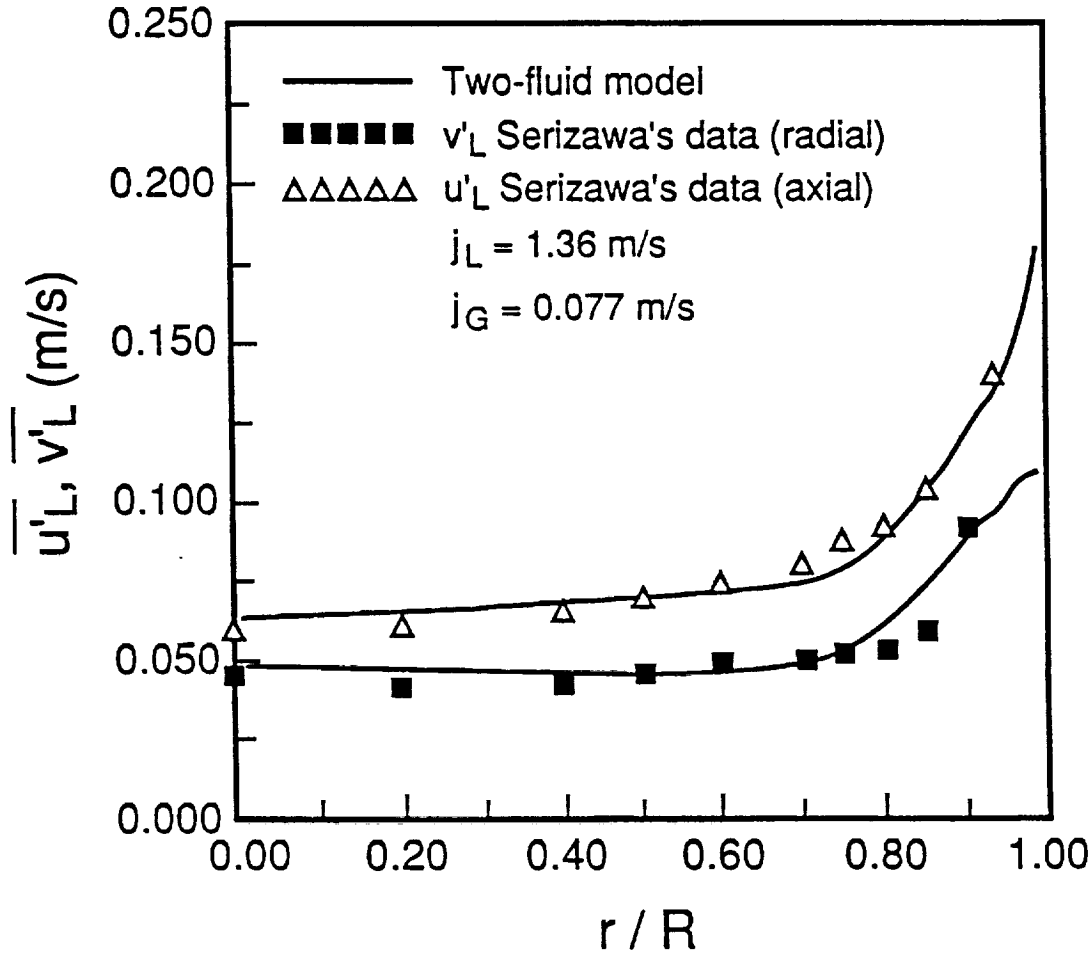

Comparison with Serizawa's data [1986]: velocity fluctuation distributions (C_L = 0.1)

Figure-2

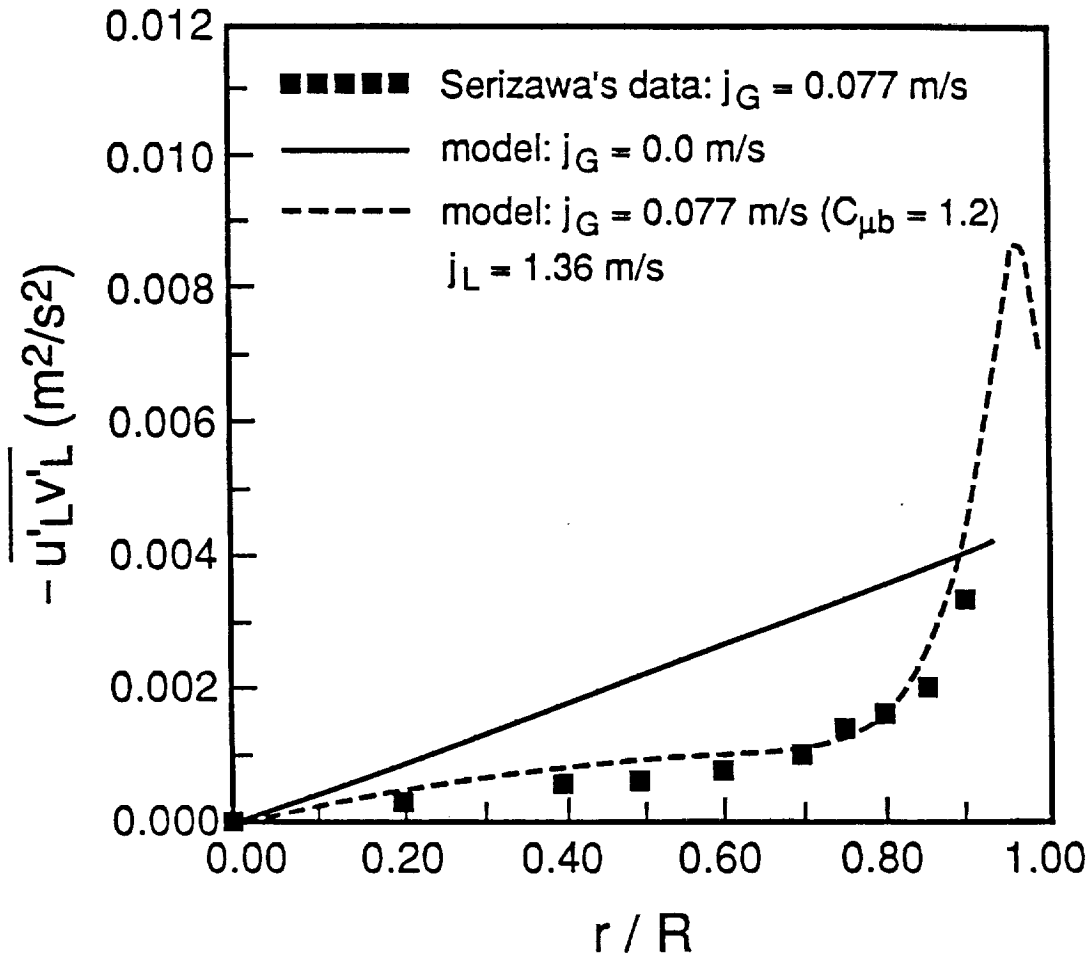

Comparison with Serizawa's data [1986]: Reynolds stress distribution (C_L = 0.1)

Figure-3

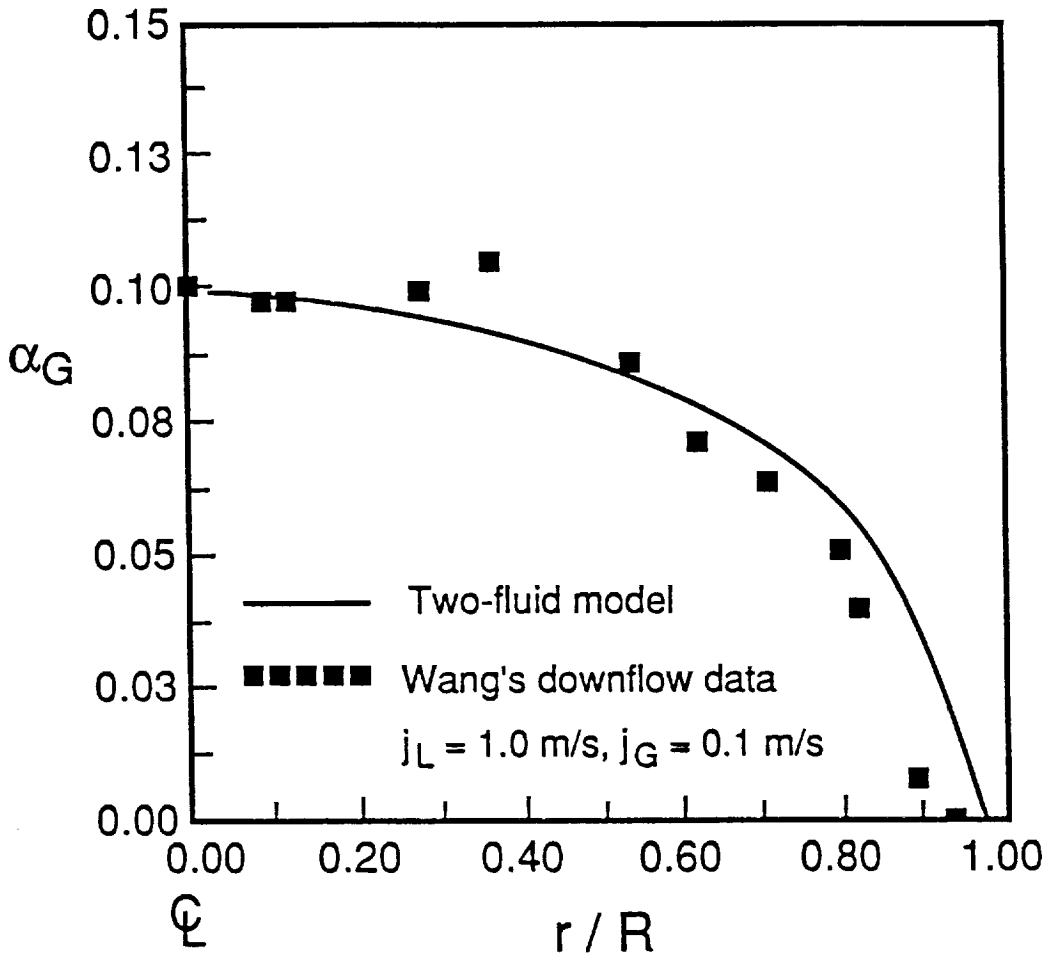

Comparison with Wang's downflow data [1986]: void fraction distribution (C_L = 0.1)

Figure-4

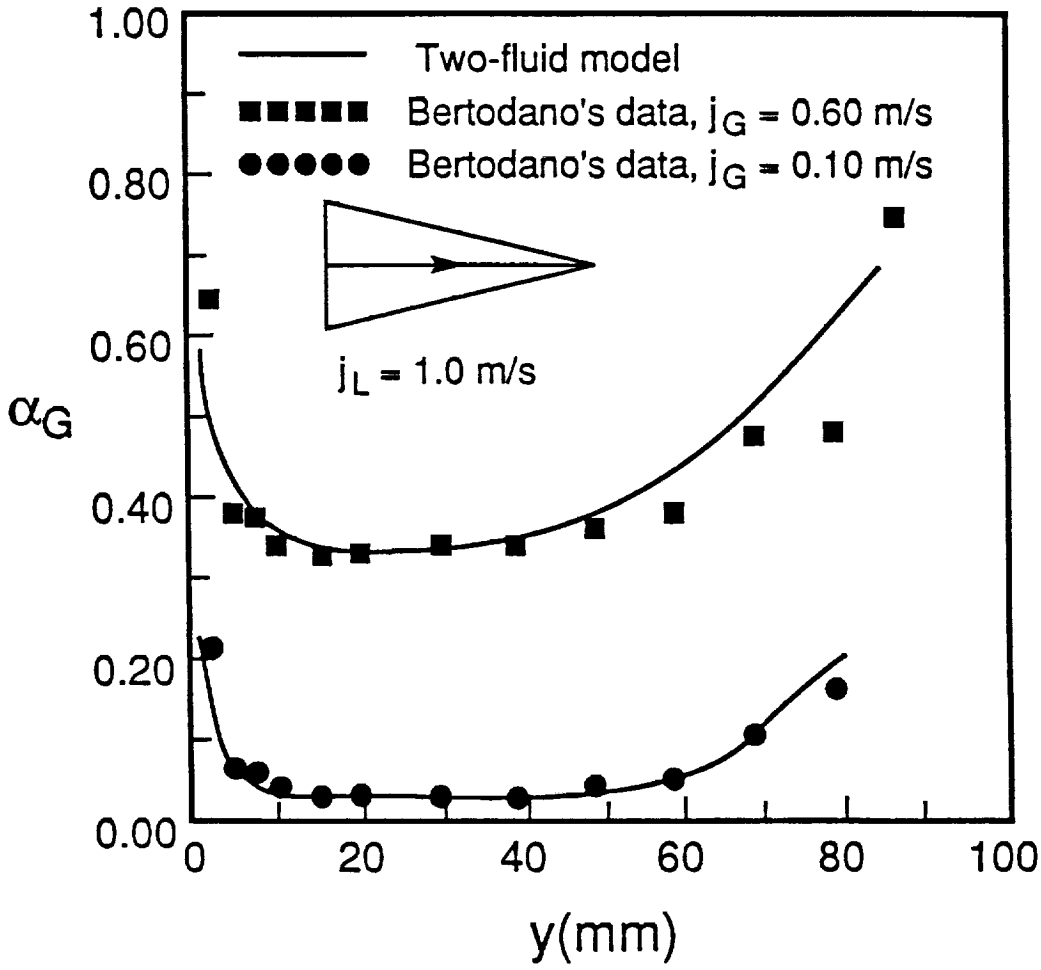

Comparison with Lopez de Bertodano's data [1992]:
void fraction distribution (C_L = 0.1)

Figure-5

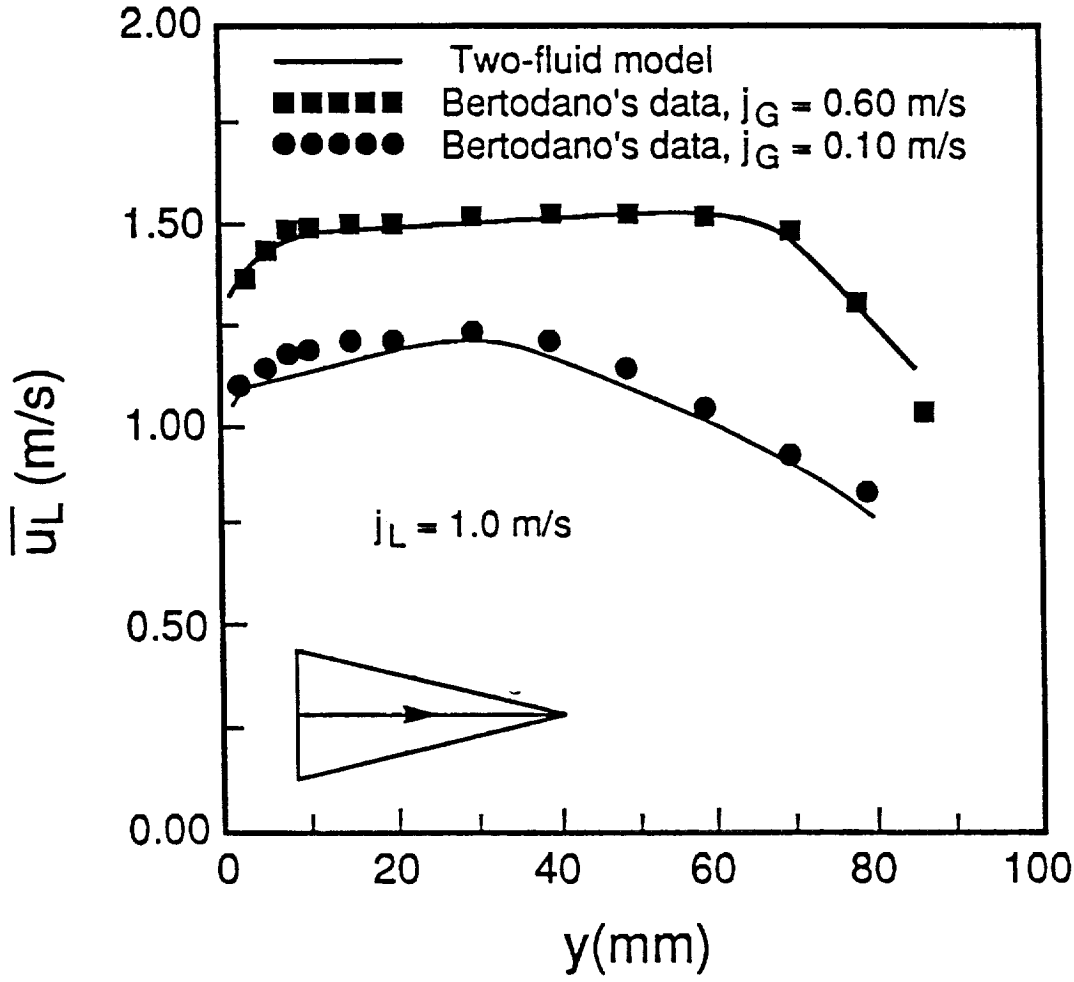

Comparison with Lopez de Bertodano's data [1992]: average axial velocity distribution (C_L = 0.1)

Figure-6

Schematic solid-liquid loop

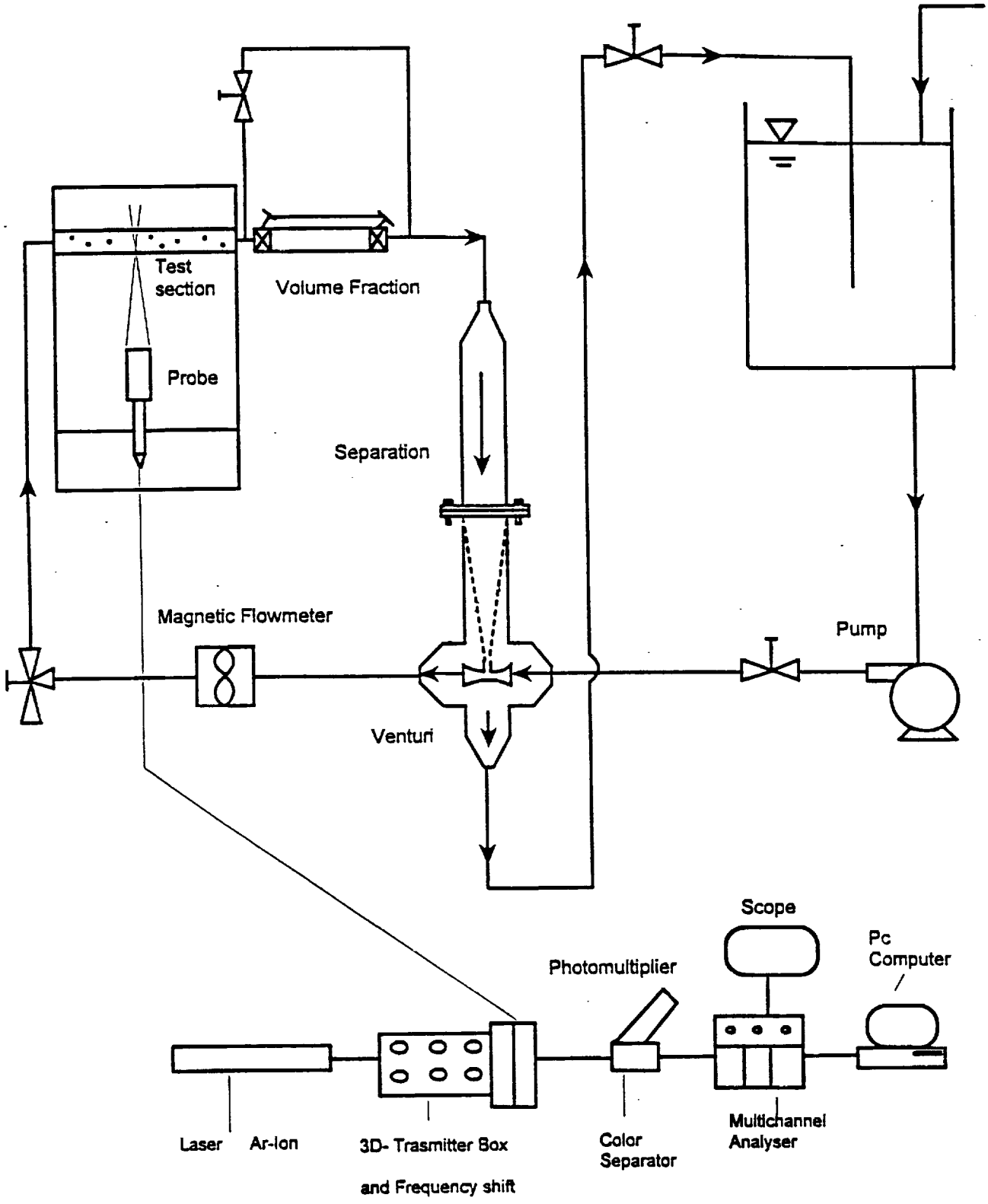

Figure-7

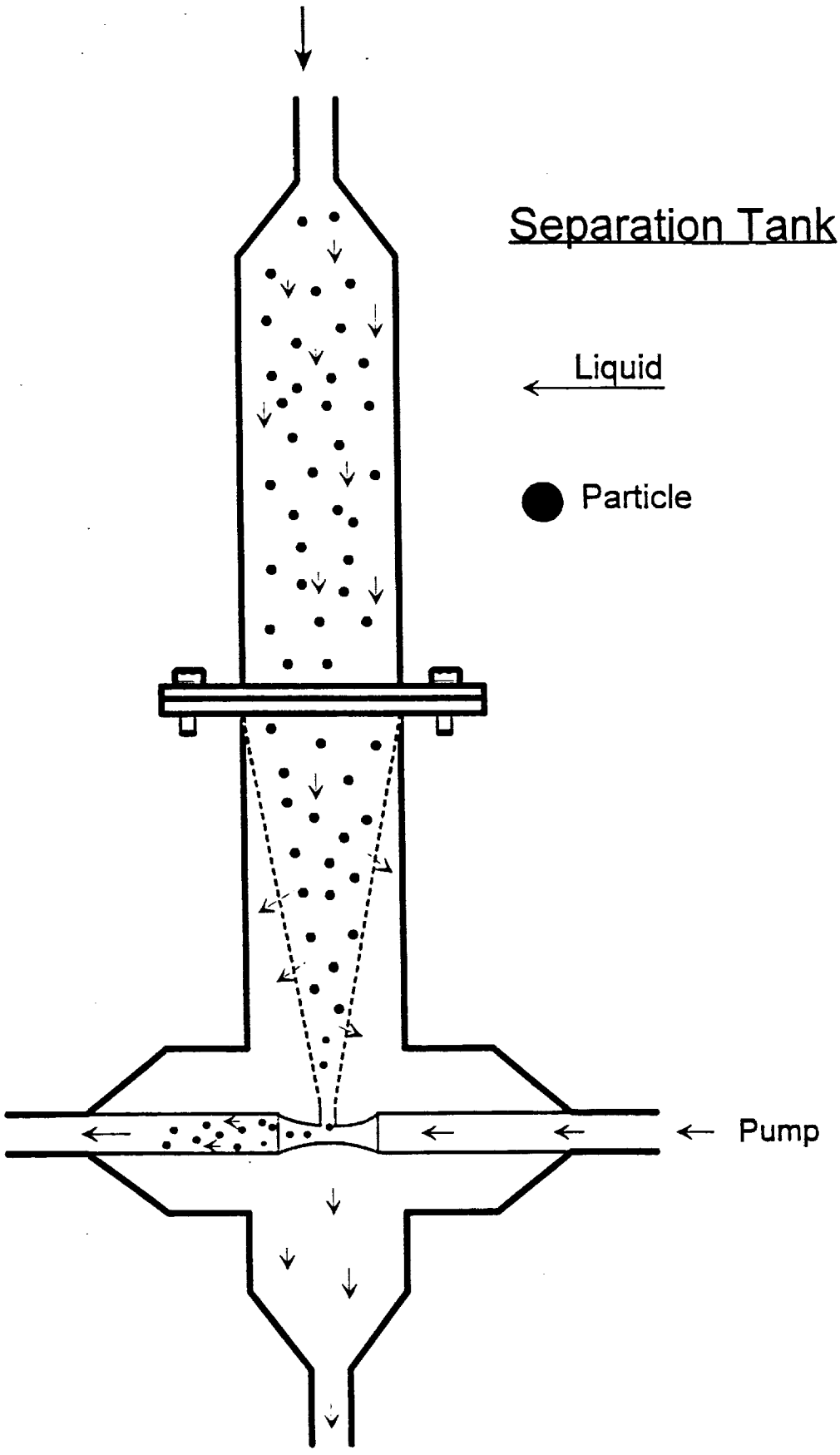

Figure-8

Experimental Setup

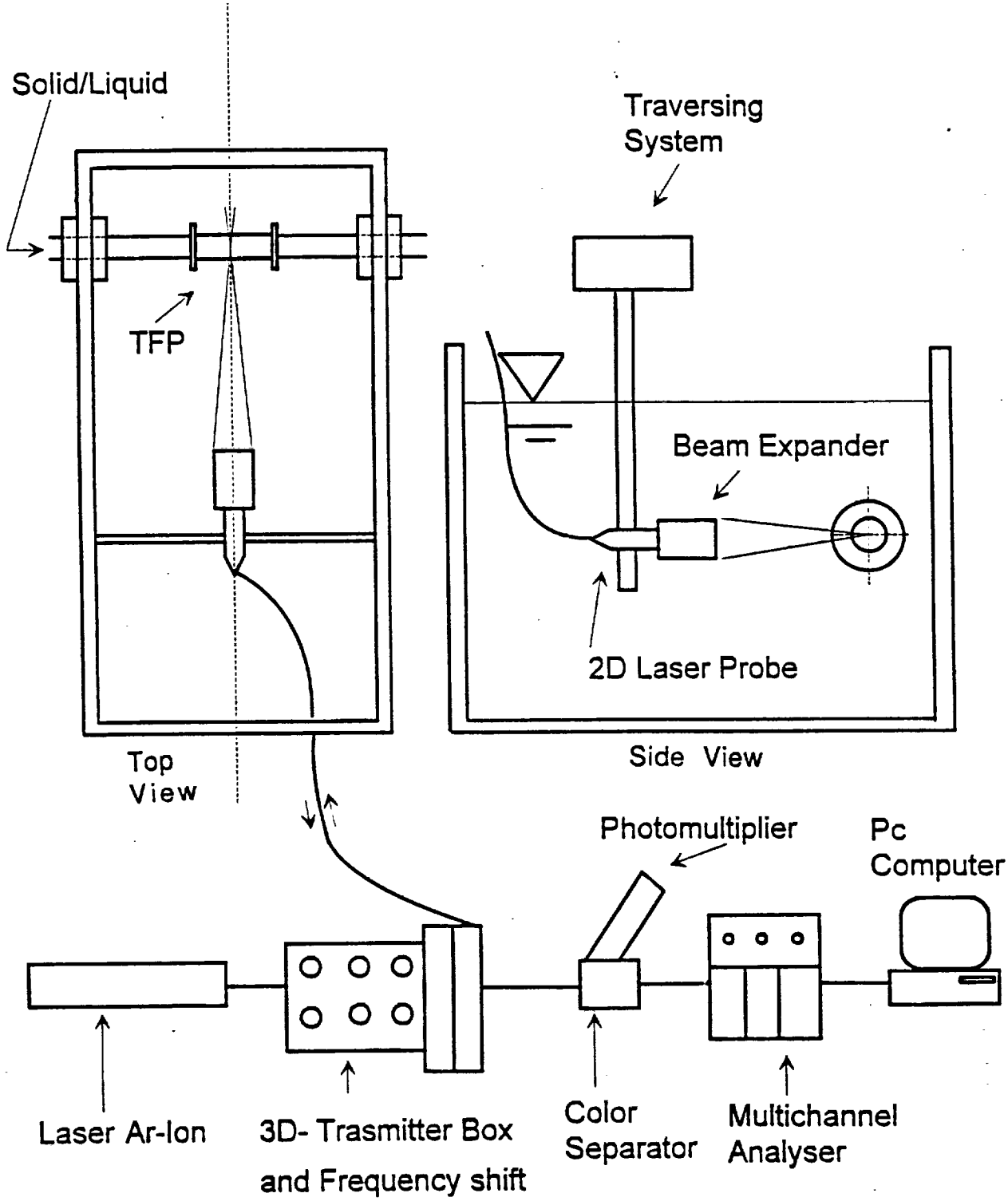

Figure-9

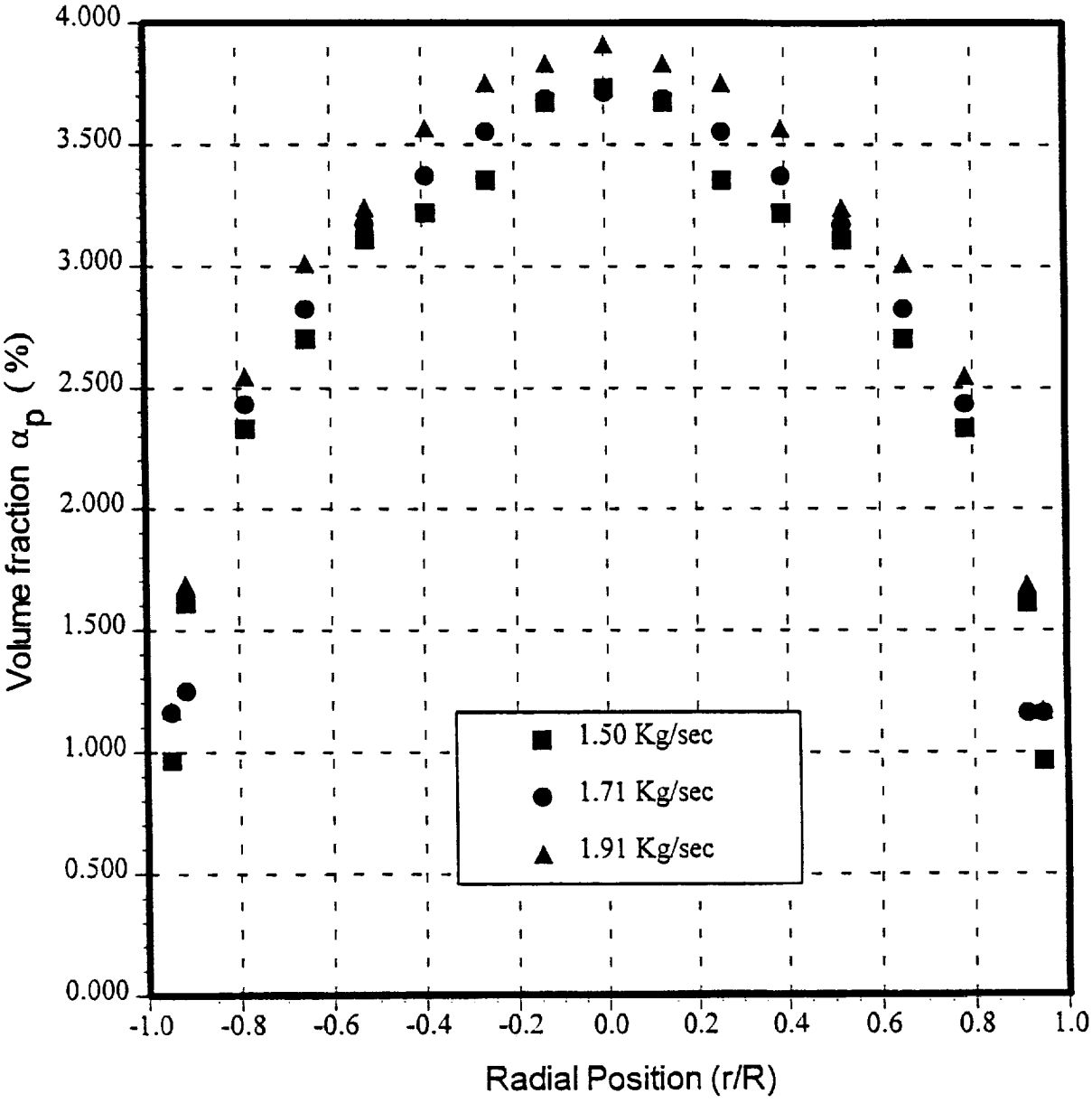

Measurement of local volume fraction for polystyrene particles with density equal to1030 Kg/m^3.

Figure - 10

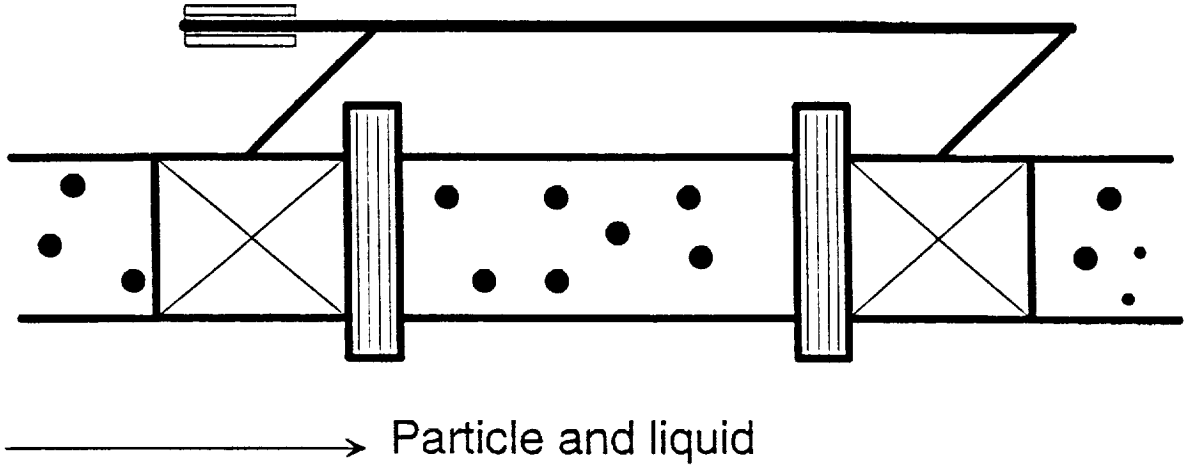

Figure-11. Quick Closing Valves

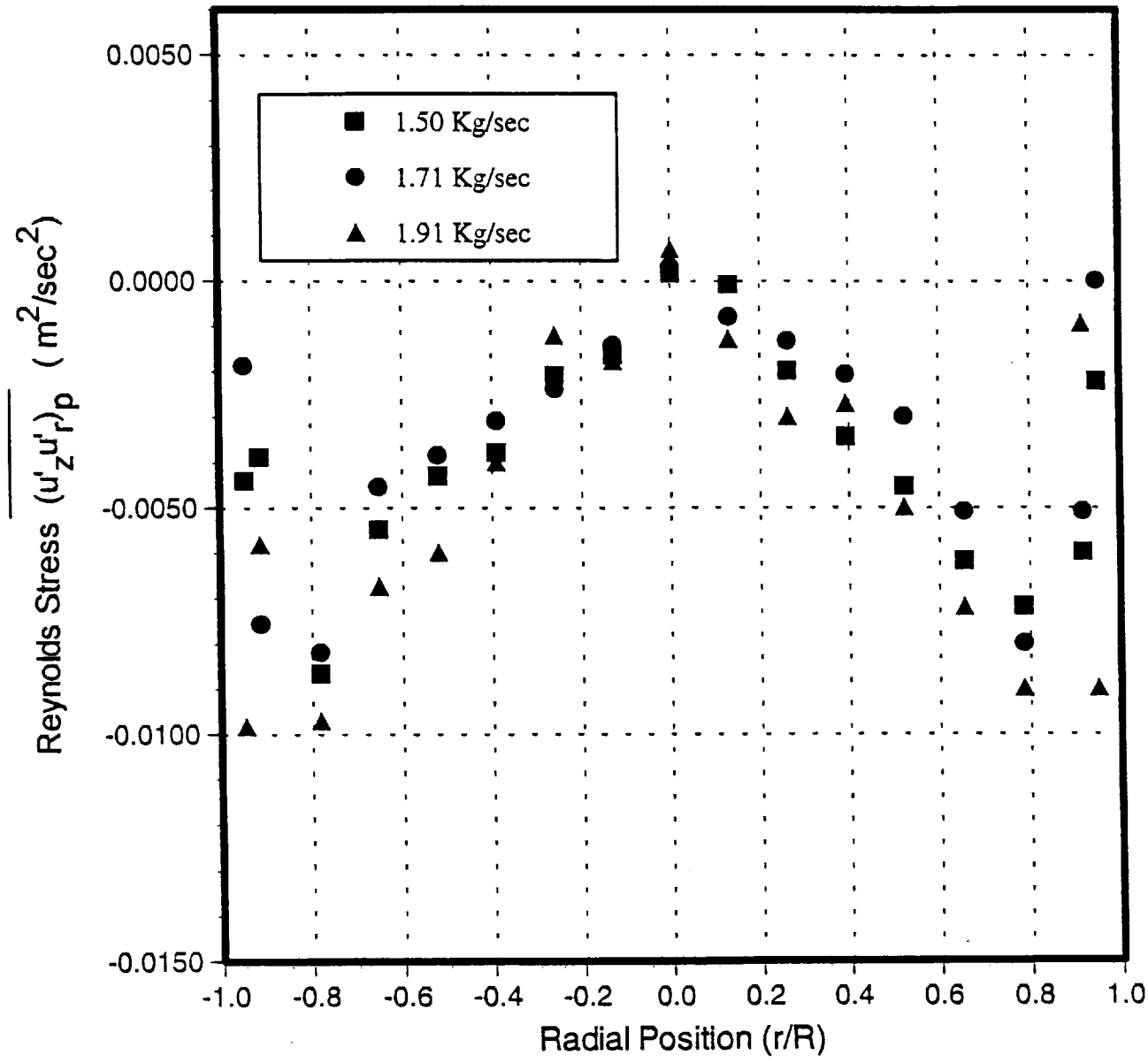

Particle Reynolds stress for polystyrene particles with density equal to 1030 Kg/m^3

Figure - 12

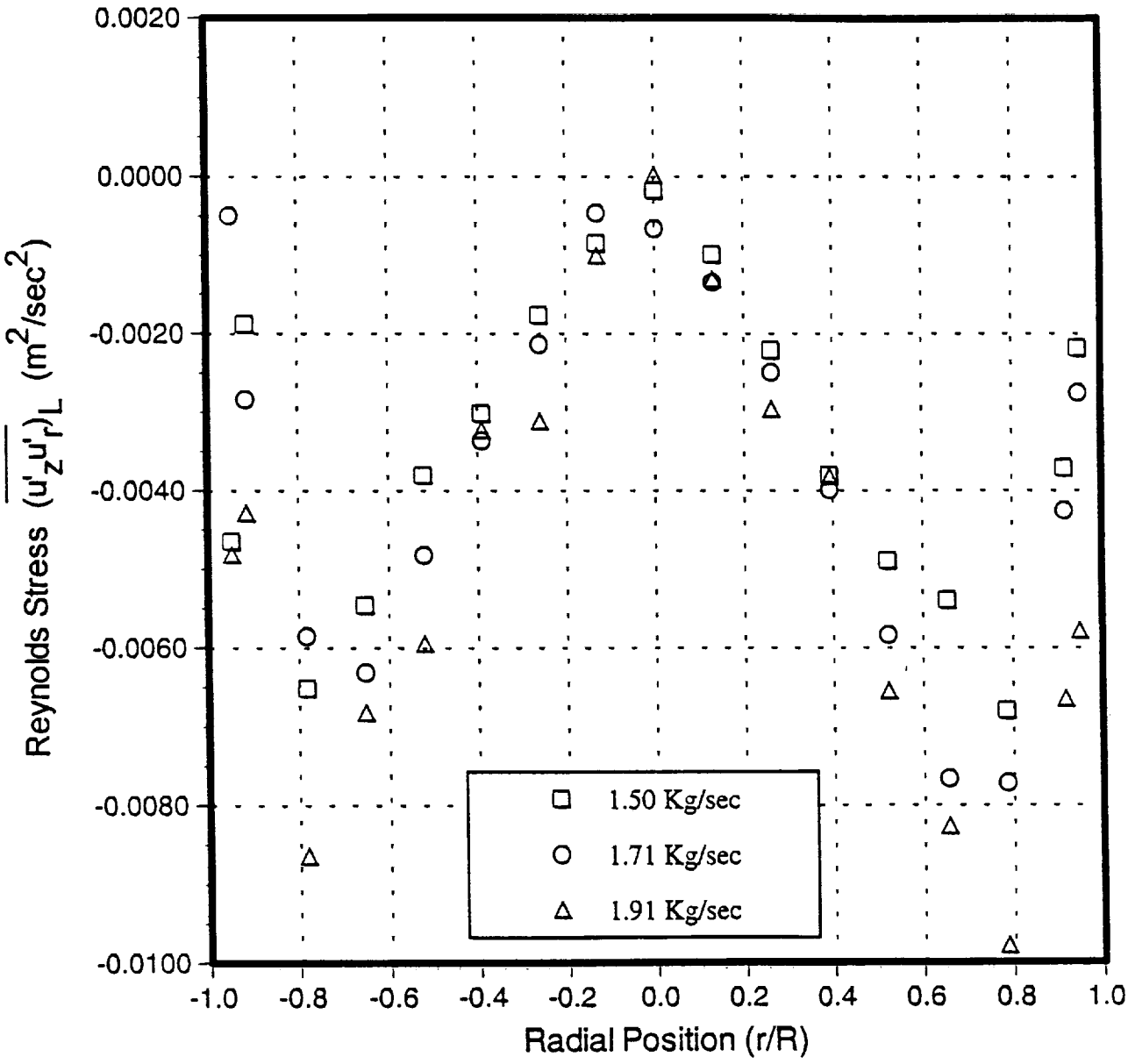

Liquid Reynolds stress for polystyrene particles with density equal to 1030 Kg/m^3

Figure - 13

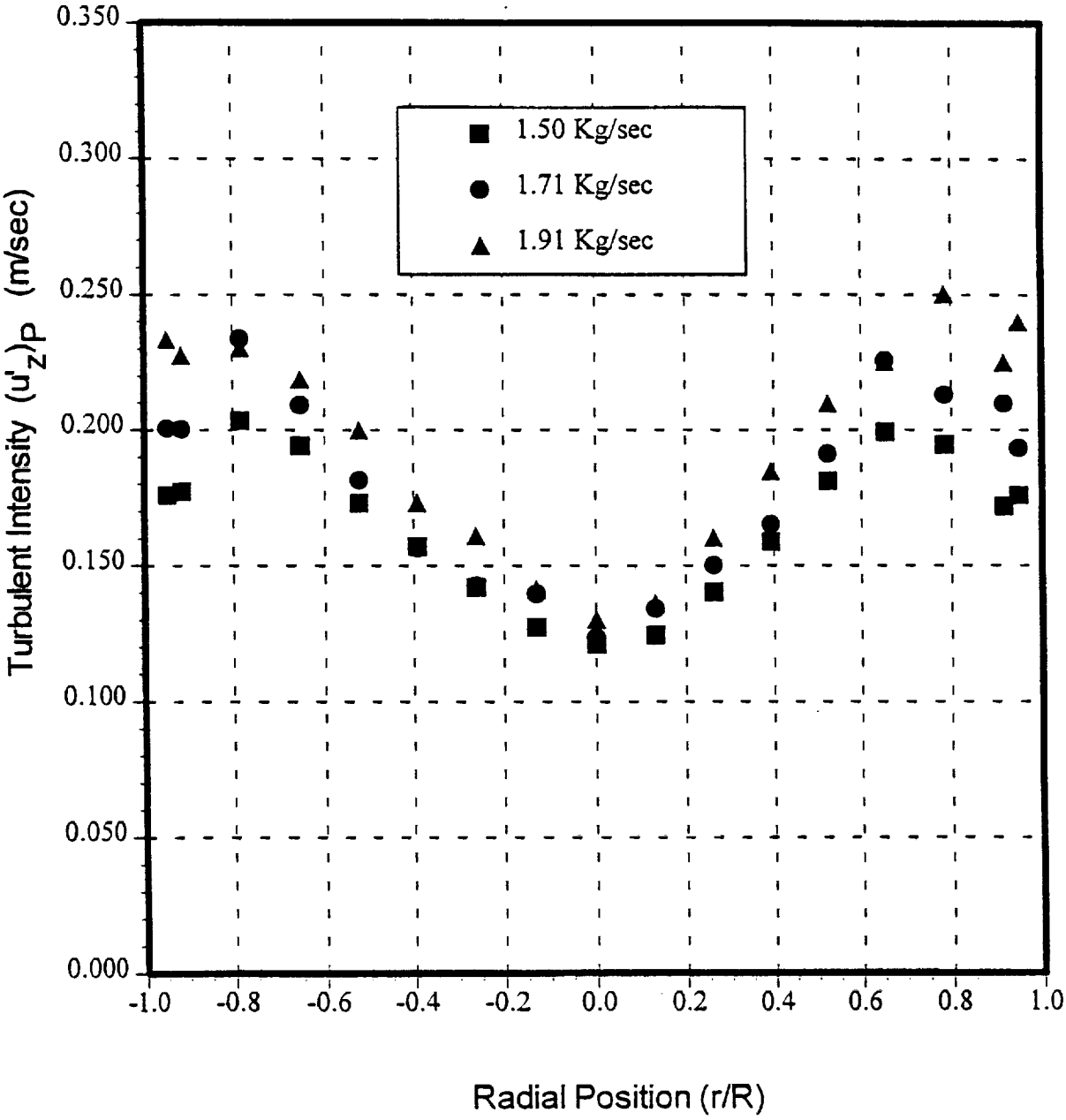

Particle axial turbulence fluctuations for polystyrene particles with density equal to 1030 Kg/m^3

Figure - 14

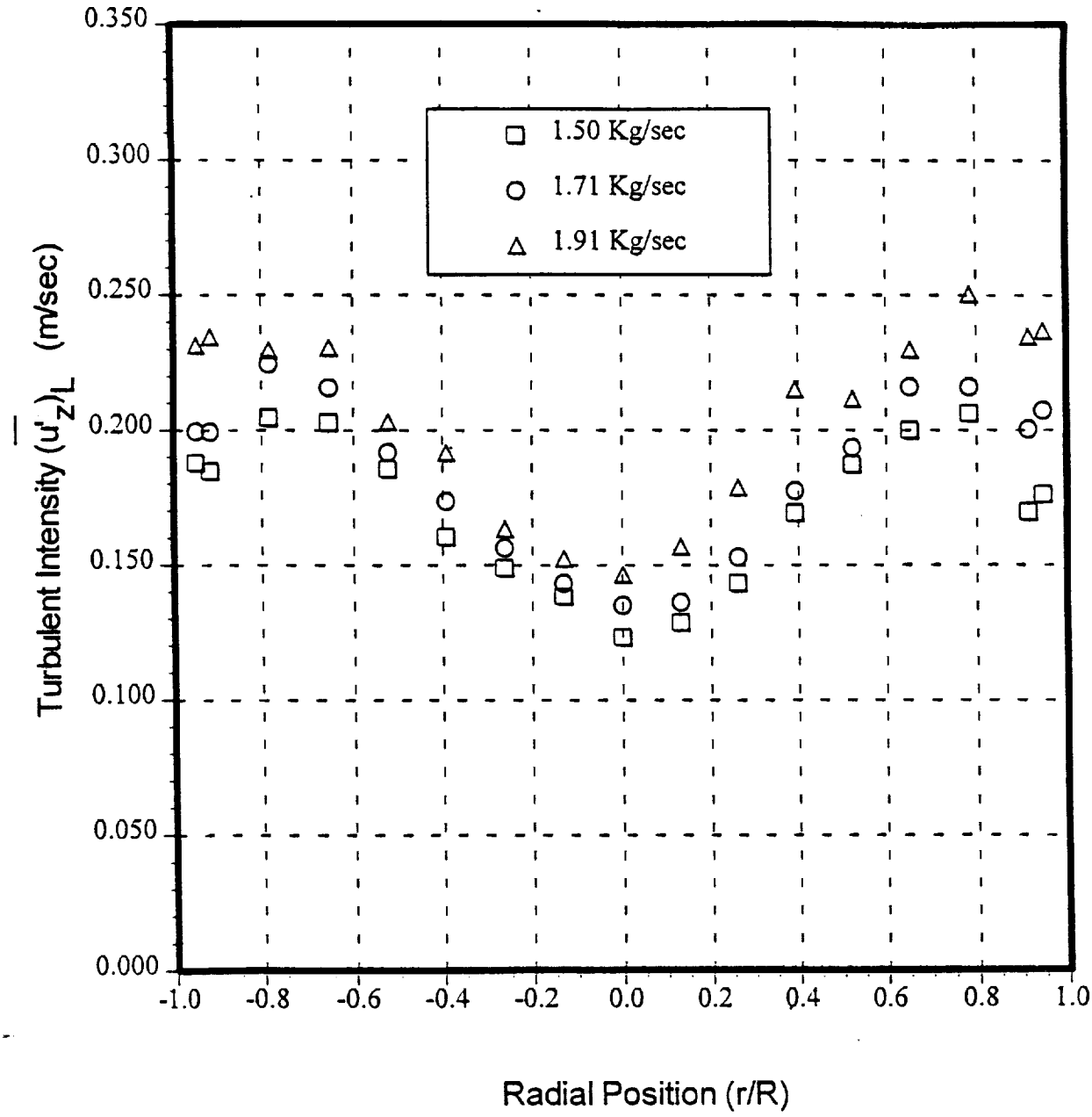

Liquid axial turbulence fuctuations for polystyrene particles with density equal to 1030 Kg/m^3

Figure - 15

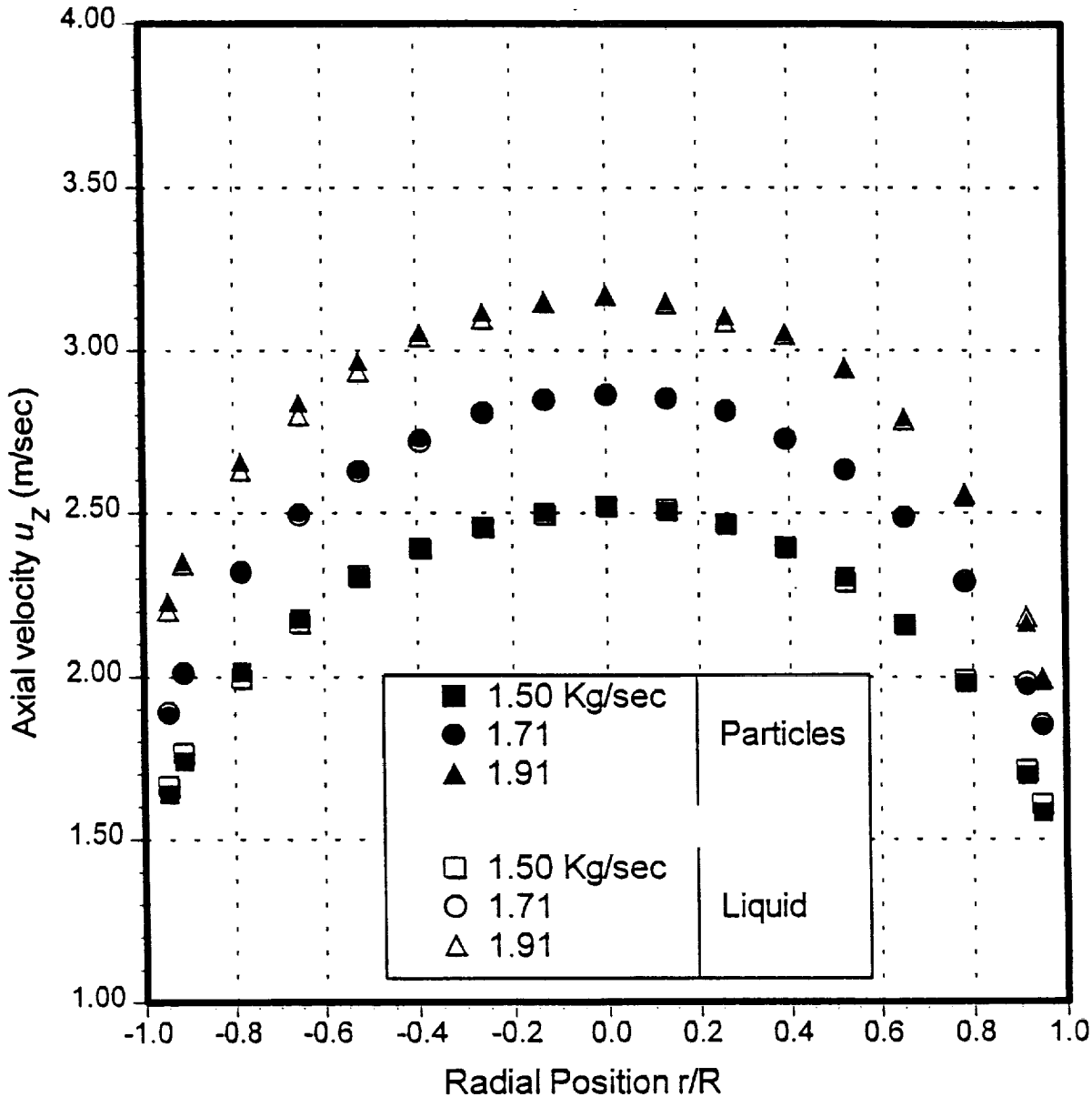

Average axial velocity for polystyrene particles with density equal to 1030.5 Kg/m^3

Figure - 16

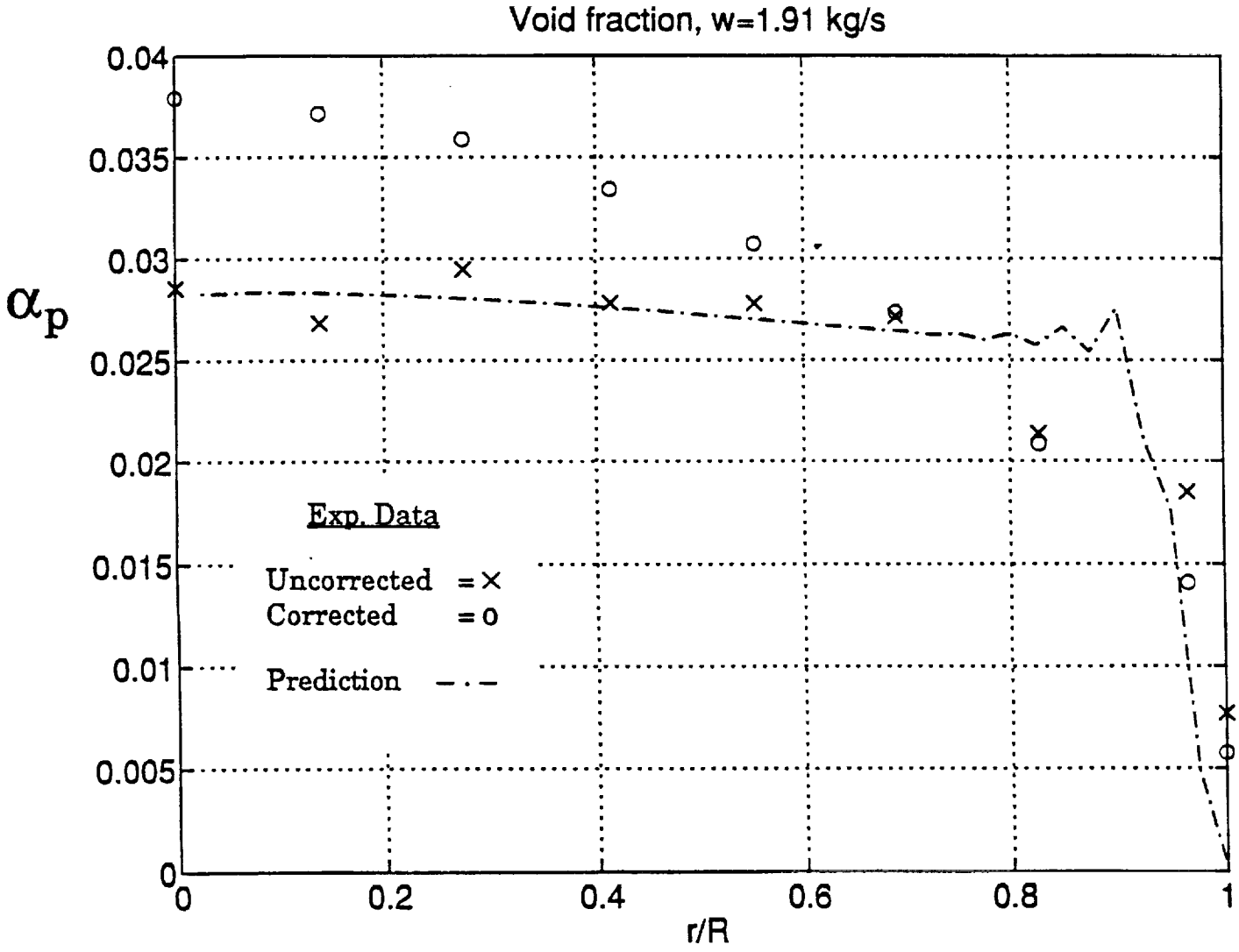

Predictions of Neutral Buoyant Particle Volume Fraction Data

Figure-17a

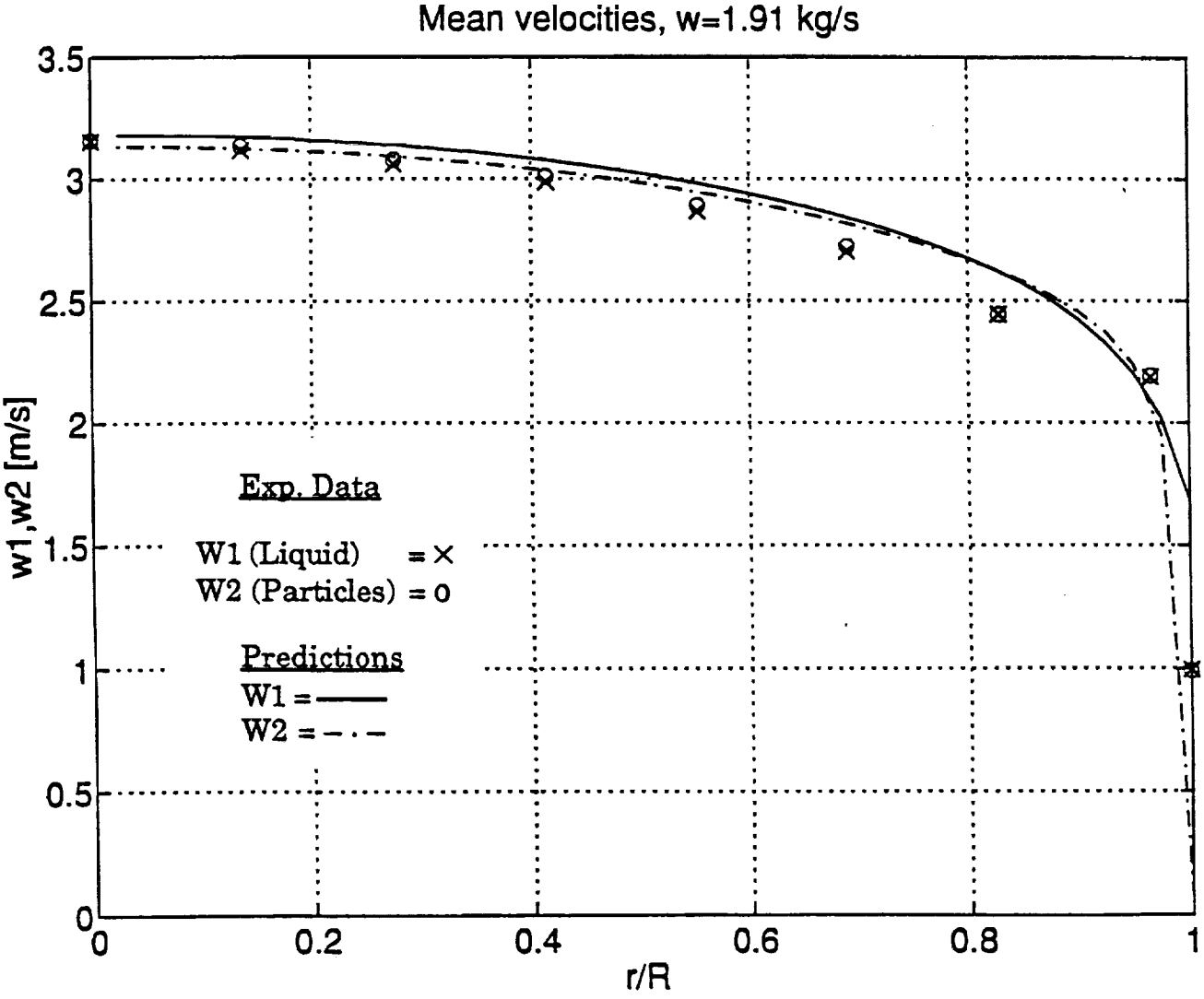

Prediction of Mean Velocity Profiles

Figure-17b

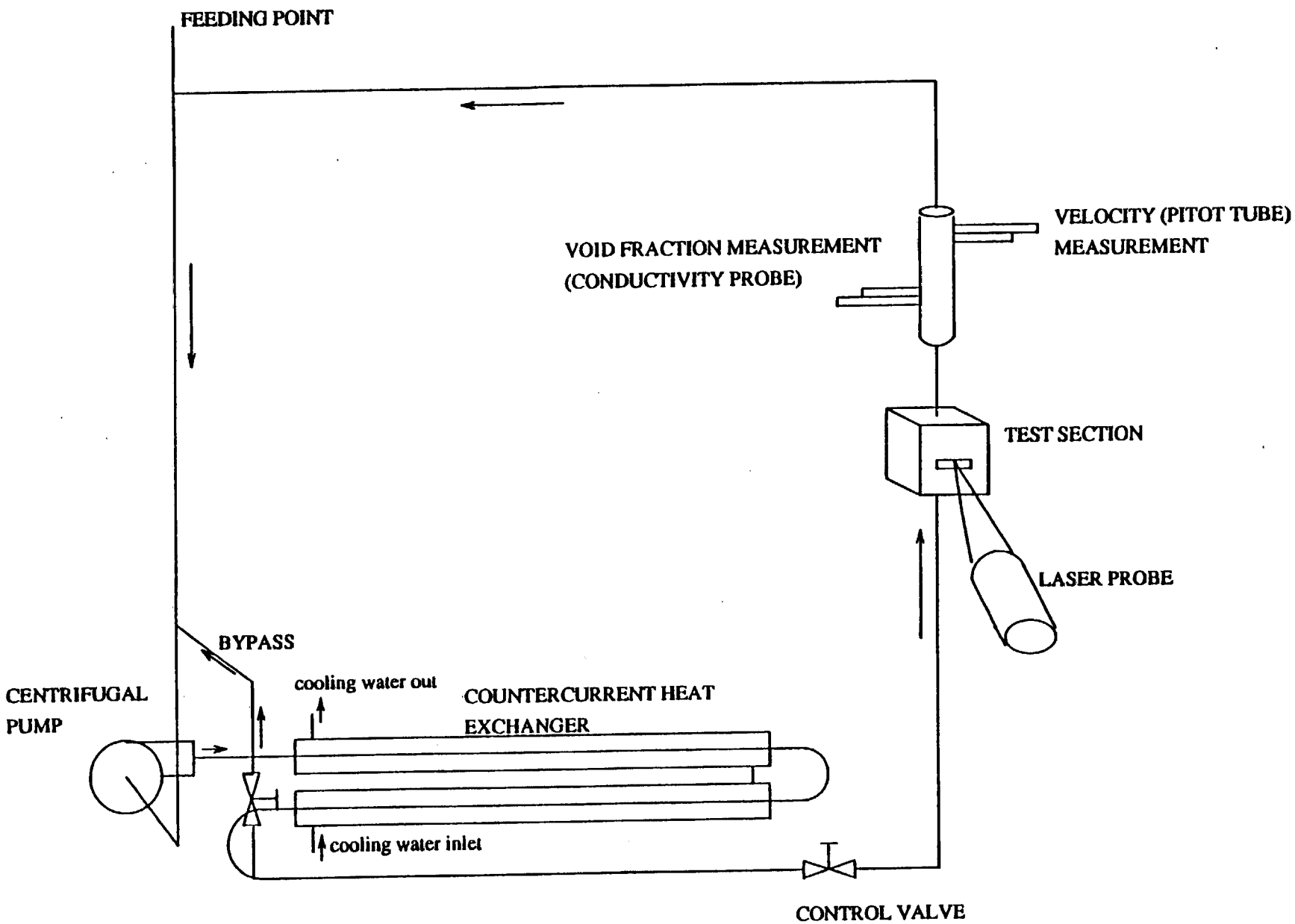

OIL/WATER LOOP

FIGURE-18